

## Bistability and Oscillations in the Bromate-Bromide-Cerium(III) System in Continuous-Flow Stirred Tank Reactor. A Simulation Using a New Set of Rate Constants of the FKN Scheme

Yoshihiro SASAKI

Institute for Chemical Research, Kyoto University, Uji, Kyoto 611

(Received June 7, 1988)

The behavior of a bromate-bromide-cerium(III) system in a continuous-flow stirred tank reactor was simulated within the framework of the FKN reaction scheme and a new set of rate constants prepared by Field and Försterling. The characteristic properties such as bistability, hysteresis and minimal oscillations could be reproduced. In order to understand bistability in this system, the dynamic behavior of a four-variable model was examined by means of a two-variable approximation.

The bromate-bromide-cerium(III) system in a sulfuric acid medium in a continuous-flow stirred tank reactor (CSTR) can possess either one or two steady states or an oscillatory state.<sup>1–4)</sup> The bistable system exists in either of the two steady states under the same set of constraints. When the system is perturbed, it relaxes to either of the two steady states, depending on the magnitude and direction of the perturbation. When the constraints are slowly changed, the system moves via a hysteresis loop between the two steady states. While the system does not contain organic substrates, it can exhibit minimal oscillations under certain conditions.

The reaction behavior of the system has been reproduced successfully through the FKN reaction scheme.<sup>2,4–9)</sup> However, it was confirmed that several rate constants in the FKN scheme are inconsistent with some kinetic studies.<sup>10–12)</sup> Therefore, Field and Försterling prepared a new set of rate constants (FF set of rate constants) on the basis of the recent results.<sup>13)</sup> The FF values are similar to the Tyson's "Lo" values.<sup>9,14)</sup> However, Bar-Eli and Ronkin found that the "Lo" values do not reproduce experiment very well, compared with the FKN values.<sup>9)</sup> Therefore, we may become interested in a computation using the FF values. In this study, the bistability and oscillations of the bromate-bromide-cerium(III) system in a CSTR were re-investigated by means of a simulation method.

### Calculations

The FKN reaction scheme can be described as follows:

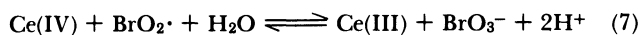
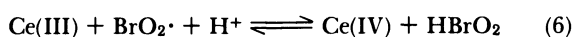
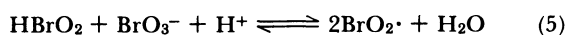
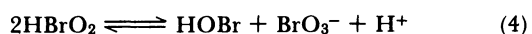
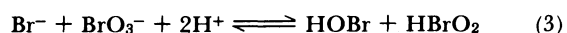
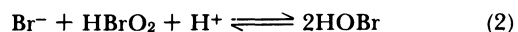
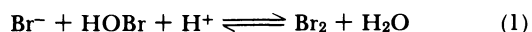


Table 1. FF Sets of Rate Constants at 20°C

Reaction	Forward	Backward
1	$8 \times 10^9 \text{ M}^{-2} \text{ s}^{-1}$	$110 \text{ s}^{-1}$
2	$3 \times 10^6 \text{ M}^{-2} \text{ s}^{-1}$	$2 \times 10^{-5} \text{ M}^{-1} \text{ s}^{-1}$
3	$2 \text{ M}^{-3} \text{ s}^{-1}$	$3.2 \text{ M}^{-1} \text{ s}^{-1}$
4	$3000 \text{ M}^{-1} \text{ s}^{-1}$	$10^{-8} \text{ M}^{-2} \text{ s}^{-1}$
5	$42 \text{ M}^{-2} \text{ s}^{-1}$	$4.2 \times 10^7 \text{ M}^{-1} \text{ s}^{-1}$
6	$8 \times 10^4 \text{ M}^{-2} \text{ s}^{-1}$	$8.9 \times 10^3 \text{ M}^{-1} \text{ s}^{-1}$
7	0	0

1 M = 1 mol dm<sup>-3</sup>.

This scheme has been used in order to explain the oxidation of cerium(III) by bromate in a sulfuric acid solution.<sup>13,15,16)</sup> The new set of rate constants at 20 °C prepared by Field and Försterling is shown in Table 1.<sup>13)</sup> When the oxidation reaction is carried out in a CSTR, the term,  $k_0(C_{0i} - C_i)$ , is added to the rate equations generated from Reactions 1–6, where  $C_i$  and  $C_{0i}$  are the concentrations of species  $i$  in the solution and in the feed flow, respectively.  $k_0$  is the ratio between the flow rate,  $dV/dt$ , and the volume of the reaction vessel. The external parameters, or constraints, for the reaction system are  $[\text{BrO}_3^-]_0$ ,  $[\text{Br}^-]_0$ ,  $[\text{Ce(III)}]_0$ ,  $[\text{H}^+]_0$ ,  $k_0$ , and the temperature.<sup>2)</sup> Therefore, the states of the system are dependent on the constraints.

In this study, the seven-variable rate equations were employed because the value of  $[\text{H}^+]_0$  was assumed to be large. The calculation of the steady states was performed by Newton's method. The temporal evolution of the system was obtained by using Gear's algorithm.<sup>17)</sup> The stability of the steady states was surveyed by means of linearized stability analysis.<sup>18)</sup>

### Results and Discussion

Figure 1 shows the relationship between  $[\text{Br}^-]_0$  and the concentration of bromide in the steady states,  $[\text{Br}^-]_{ss}$ , when  $[\text{H}^+]_0 = 1.5 \text{ mol dm}^{-3}$ ,  $[\text{Ce(III)}]_0 = 1.5 \times 10^{-4} \text{ mol dm}^{-3}$  and  $k_0 = 0.004 \text{ s}^{-1}$ . The state of the reaction system depended on the concentration of bromate in the feed flow. That is, when  $[\text{BrO}_3^-]_0 \leq 6 \times 10^{-5} \text{ mol dm}^{-3}$ , the system existed in ssI, which was characterized by a relatively high  $[\text{Br}^-]_{ss}$  and a low  $[\text{Ce(IV)}]_{ss}$ .

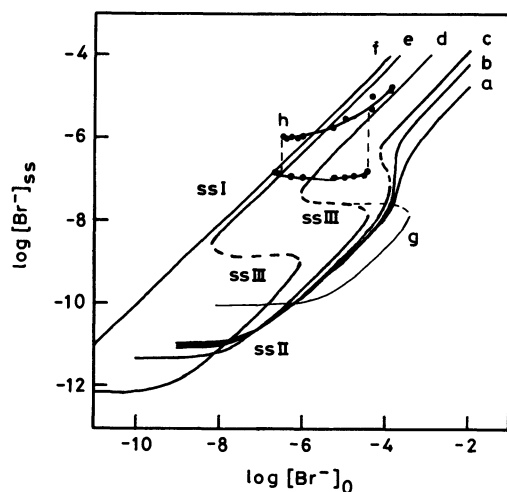


Fig. 1. Relationship between  $[\text{Br}^-]_0$  and  $[\text{Br}^-]_{ss}$ .  $[\text{Ce(III)}]_0 = 1.5 \times 10^{-4} \text{ M}$ ,  $[\text{H}^+]_0 = 1.5 \text{ M}$ , and  $k_0 = 0.004 \text{ s}^{-1}$ .  $[\text{BrO}_3^-]_0$  (M) a: 0.1, b: 0.032, c: 0.016, d: 0.002, e:  $2 \times 10^{-4}$ , f:  $5 \times 10^{-5}$ . g: calculated according to the four-variable model under the same conditions in d. h: experimental results at  $25^\circ\text{C}$  under the same conditions in d.<sup>2)</sup>

When  $[\text{BrO}_3^-]_0 \geq 0.032 \text{ mol dm}^{-3}$ , the steady state of the system varied smoothly from ssI to ssII (low concentration of bromide and high concentration of cerium(IV)) with a decrease of  $[\text{Br}^-]_0$ . On the other hand, when  $7.5 \times 10^{-5} \text{ mol dm}^{-3} \leq [\text{BrO}_3^-]_0 \leq 2.2 \times 10^{-2} \text{ mol dm}^{-3}$ , the system could possess three steady states (ssI, ssII, and ssIII) under the same set of  $[\text{BrO}_3^-]_0$  and  $[\text{Br}^-]_0$ . The steady states (ssI and ssII) were stable and had all the negative eigen-values (nodes). The steady state (ssIII) was unstable and had one positive and the other negative eigenvalues (saddle point). These results mean that we can not attain ssIII experimentally and that the system exists in either ssI or ssII. Also, if  $[\text{Br}^-]_0$  is continually changed to a slightly different value, the system in one steady state suddenly moves to the other steady state at a critical value of  $[\text{Br}^-]_0$ . Thus, we obtain a hysteresis loop. The calculated curve, d, was not consistent with the experimental results at  $25^\circ\text{C}$  due to Geiseler and Bar-Eli<sup>2)</sup> in the region of low bromide-concentration. The inconsistency may be attributed to a difficulty involving the determination of bromide in the region by means of a bromide-sensitive electrode.<sup>19)</sup> However, the dynamical behavior, such as bistability and hysteresis, could be reproduced successfully.

Figure 2 shows the calculated hysteresis limits together with the experimental results due to Geiseler and Bar-Eli.<sup>2)</sup> The bistable region of the system lays in a five-dimensional space of  $[\text{BrO}_3^-]_0$ ,  $[\text{Ce(III)}]_0$ ,  $[\text{H}^+]_0$ ,  $[\text{Br}^-]_0$ , and  $k_0$ . Four of 10 two-dimensional subspaces were examined in this study. In the figure, the system existed in ssII below the lower lines and in ssI above the upper lines, respectively. In the intermediate region, the two steady states coexisted. All of the

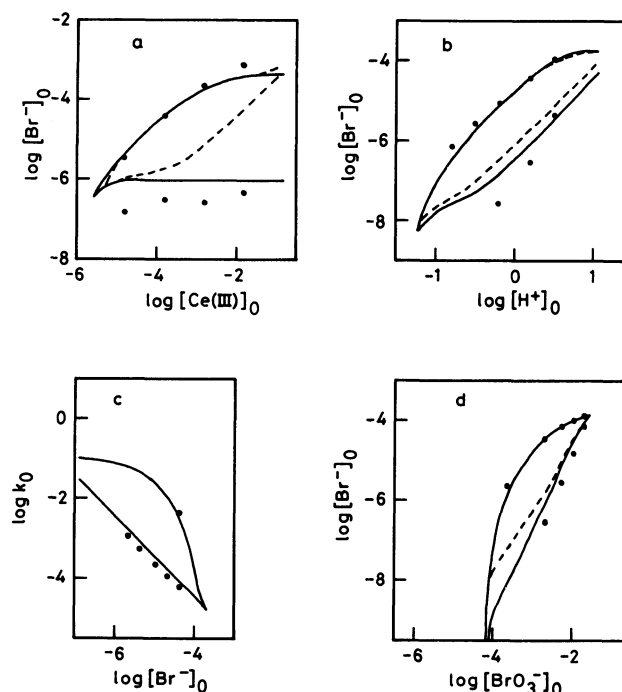


Fig. 2. Hysteresis limits. Solid lines: calculated, points: experimental ( $25^\circ\text{C}$ ).<sup>2)</sup> dashed lines: calculated when  $k_{-7} = 0.001 \text{ M}^{-3} \text{ s}^{-1}$ . Subspaces and fixed constraints a:  $[\text{Ce(III)}]_0$ - $[\text{Br}^-]_0$ ,  $[\text{BrO}_3^-]_0 = 0.002 \text{ M}$ ,  $[\text{H}^+]_0 = 1.5 \text{ M}$ ,  $k_0 = 0.004 \text{ s}^{-1}$ ; b:  $[\text{H}^+]_0$ - $[\text{Br}^-]_0$ ,  $[\text{BrO}_3^-]_0 = 0.002 \text{ M}$ ,  $[\text{Ce(III)}]_0 = 1.5 \times 10^{-4} \text{ M}$ ,  $k_0 = 0.004 \text{ s}^{-1}$ ; c:  $[\text{Br}^-]_0$ - $k_0$ ,  $[\text{BrO}_3^-]_0 = 0.002 \text{ M}$ ,  $[\text{Ce(III)}]_0 = 1.5 \times 10^{-4} \text{ M}$ ,  $[\text{H}^+]_0 = 1.5 \text{ M}$ ; d:  $[\text{BrO}_3^-]_0$ - $[\text{Br}^-]_0$ ,  $[\text{Ce(III)}]_0 = 1.5 \times 10^{-4} \text{ M}$ ,  $[\text{H}^+]_0 = 1.5 \text{ M}$ ,  $k_0 = 0.004 \text{ s}^{-1}$ .

upper lines were consistent with the experimental data. However, the lower lines deviated slightly from the experimental data. The reason for the deviation is not apparent at present.

The bromate-bromide-cerium(III) system which we studied possessed a small oscillation region in the neighborhood of the bistable domain. Figure 3 shows the oscillation region projected on the  $[\text{BrO}_3^-]_0$ - $[\text{Br}^-]_0$  subspace, where a represents an oscillation domain having one unstable steady state ( $\text{Re}(\lambda) > 0$ ) and b denotes a bistable region. In regions c and d, there were three steady states (one saddle point, one stable node and one unstable steady state ( $\text{Re}(\lambda) > 0$ )). The system then settled in a stable node after a long time. However, in the domain where c and d were piled up, three unstable states were obtained and the system exhibited one limit cycle. In the other region of Fig. 3, one stable steady state existed. The region, a, calculated here seems to reproduce the experimental oscillation region at  $25^\circ\text{C}$ , e, due to Bar-Eli and Geiseler in location, size and shape.<sup>4)</sup> The oscillation period and the ratio,  $[\text{Br}^-]_{\text{max}}/[\text{Br}^-]_{\text{min}}$ , calculated are shown in Table 2. At high  $[\text{BrO}_3^-]_0$  and  $[\text{Br}^-]_0$ , the amplitude and the period were comparably small and at low  $[\text{BrO}_3^-]_0$  and  $[\text{Br}^-]_0$ , comparably large. A similar trend was obtained experimentally.<sup>4)</sup> The

Table 2. Period and Amplitude of the Oscillations

$[\text{BrO}_3^-]_0/\text{M}$	$[\text{Br}^-]_0/\text{M}$	Period/s	$[\text{Br}^-]_{\text{max}}/[\text{Br}^-]_{\text{min}}$
0.116	$3.2 \times 10^{-4}$	307	2.5
0.11	$3.1 \times 10^{-4}$	345	3.5
0.10	$2.8 \times 10^{-4}$	370	6.4
0.09	$2.65 \times 10^{-4}$	445	11.3
0.082	$2.45 \times 10^{-4}$	643	17.3
0.078	$2.37 \times 10^{-4}$	905	22.3

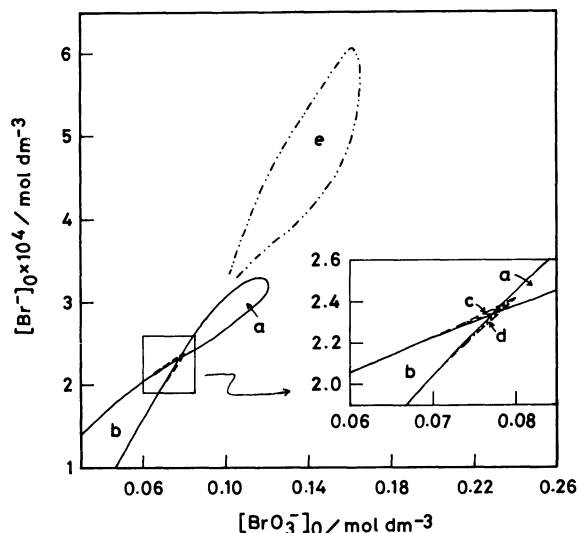


Fig. 3. Oscillation and bistability regions in the  $[\text{BrO}_3^-]_0$ - $[\text{Br}^-]_0$  subspace.  $[\text{H}^+]_0 = 0.75 \text{ M}$ ,  $[\text{Ce(III)}]_0 = 3 \times 10^{-4} \text{ M}$ , and  $k_0 = 0.005 \text{ s}^{-1}$ . a: oscillation, b: bistability, c and d: regions having one stable and two unstable steady states e: experimental oscillation region at  $25^\circ\text{C}$ .<sup>4)</sup> The domain where c and d intersect has three unstable steady states.

magnitudes of the oscillation period and the amplitude were also consistent with the experiment (the oscillation period: 156–493 s and the amplitude: 1.6–15).

The FF set of rate constants, prepared on the basis of recent kinetic data, reproduces the reaction behavior of the bromate-bromide-cerium(III) system well, as is shown in Figs. 1–3. In the calculation, the contribution of Reaction 7 is not taken into account due to Field and Försterling, who assumed that a small quantity of bromide remaining as an impurity in bromate is a trigger for the oxidation of Ce(III) by bromate in a sulfuric acid medium. It is reported that the induced period varies in the oxidation of Ce(III) ( $3 \times 10^{-4} \text{ mol dm}^{-3}$ ) by  $0.001 \text{ mol dm}^{-3}$  of bromate,<sup>20)</sup> which may support the assumption by Field and Försterling.

However, Reaction 7 is a conceivable trigger for the oxidation of Ce(III) by bromate. Therefore, in order to examine the contribution of Reaction 7, we simulated the observed  $[\text{Ce(IV)}]$  and  $[\text{BrO}_2\cdot]$  during the overall reaction of Ce(III) with bromate and the hysteresis limits by taking account of the reaction. The

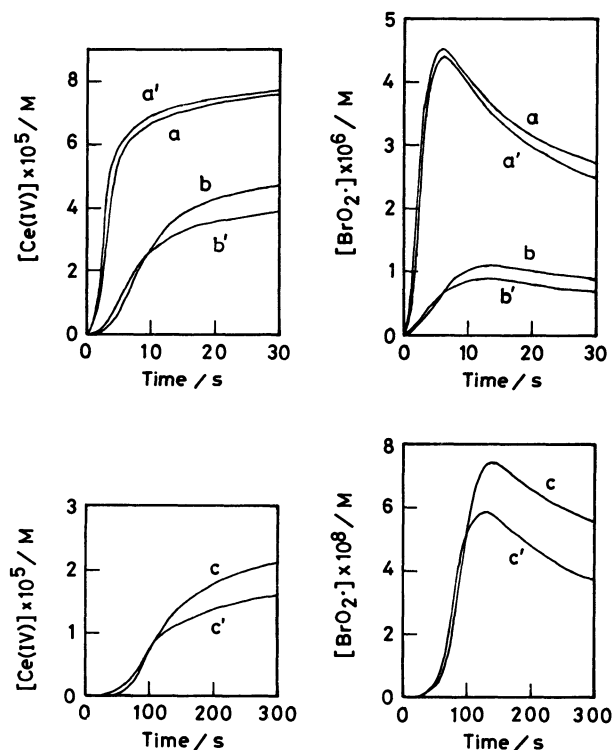
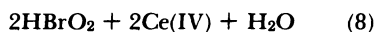
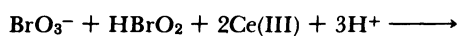


Fig. 4. Simulations of  $[\text{Ce(IV)}]$  and  $[\text{BrO}_2\cdot]$  in the oxidation reaction of Ce(III) with bromate in 1 M sulfuric acid solution.  $[\text{H}^+]_{\text{initial}} = 1 \text{ M}$ ,  $[\text{Ce(III)}]_{\text{initial}} = 10^{-4} \text{ M}$ .  $[\text{BrO}_3^-]_{\text{initial}} (\text{M})$ : a: 1, b: 0.1, c: 0.002. The prime represents the experiment due to Field and Försterling.<sup>13)</sup>

unknown value of  $k_{-7}$  was estimated by trial and  $k_7$  was obtained according to the relationship,  $k_5 k_6 k_{-7} = k_{-5} k_{-6} k_7$ . Figure 4 shows the calculated concentrations of Ce(IV) and  $\text{BrO}_2\cdot$  when  $k_{-7} = 0.001 \text{ mol}^{-3} \text{ dm}^9 \text{ s}^{-1}$ . The calculated curves in Fig. 4 were consistent with the experimental results due to Field and Försterling.<sup>13)</sup> The hysteresis limits calculated when  $k_{-7} = 0.001 \text{ mol}^{-3} \text{ dm}^9 \text{ s}^{-1}$  are shown in Figs. 2a, b, and d. Reaction 7 influenced mainly the lower lines, especially in the regions of relatively large  $[\text{Ce(III)}]_0$  and small  $[\text{BrO}_3^-]_0$ . Figures 2a, b, and d suggest that the contribution of Reaction 7 to the behavior of the bromate-bromide-cerium(III) system in a CSTR is not so large.

As is described above, a bromate-bromide-cerium(III) system kept far from thermodynamic equilibrium can possess two steady states under the same set of

constraints. The behavior is based on the autocatalytic formation of  $\text{HBrO}_2$  by Reactions 5 and 6, and based on competition between Reactions 2 and 5. However, because this explanation is not sufficient to understand the properties of the system, we examined the dynamical behavior of a four-variable model composed of Reactions 1–4 and 8.



Reaction 8 is obtained when the backward reactions in Reactions 5 and 6 are neglected. In this model, Reaction 5 is assumed to be rate determining in the autocatalytic reaction. Such a condition can be realized when  $[\text{Ce(III)}]_0$  is very large. Thus, the rate of Reaction 8 is yielded as follows:

$$v_8 = k_5[\text{H}^+]_0[\text{BrO}_3^-][\text{HBrO}_2] \quad (9)$$

Because the bromate–bromide–cerium(III) system studied here contains a large excess of bromate,  $[\text{BrO}_3^-]$  is substantially equal to  $[\text{BrO}_3^-]_0$  and the backward reactions in Reactions 2 and 4 can be neglected. The state of the model system depends on four constraints,  $[\text{H}^+]_0$ ,  $[\text{BrO}_3^-]_0$ ,  $[\text{Br}^-]_0$ , and  $k_0$ .

The rate equations generated from the four-variable model are written as follows:

$$d[\text{Br}_2]/dt = k_1[\text{H}^+]_0[\text{Br}^-][\text{HOBr}] - (k_0 + k_{-1})[\text{Br}_2] \quad (10)$$

$$\begin{aligned} d[\text{HBrO}_2]/dt = & k_3[\text{H}^+]_0^2[\text{BrO}_3^-]_0[\text{Br}^-] - k_{-3}[\text{HOBr}][\text{HBrO}_2] \\ & - k_2[\text{H}^+]_0[\text{Br}^-][\text{HBrO}_2] + k_5[\text{H}^+]_0[\text{BrO}_3^-]_0[\text{HBrO}_2] \\ & - 2k_4[\text{HBrO}_2]^2 - k_0[\text{HBrO}_2] \end{aligned} \quad (11)$$

$$\begin{aligned} d[\text{HOBr}]/dt = & k_3[\text{H}^+]_0^2[\text{BrO}_3^-]_0[\text{Br}^-] - k_{-3}[\text{HOBr}][\text{HBrO}_2] \\ & + k_{-1}[\text{Br}_2] - k_1[\text{H}^+]_0[\text{Br}^-][\text{HOBr}] \\ & + 2k_2[\text{H}^+]_0[\text{Br}^-][\text{HBrO}_2] + k_4[\text{HBrO}_2]^2 - k_0[\text{HOBr}] \end{aligned} \quad (12)$$

$$\begin{aligned} d[\text{Br}^-]/dt = & k_{-3}[\text{HOBr}][\text{HBrO}_2] - k_3[\text{H}^+]_0^2[\text{BrO}_3^-]_0[\text{Br}^-] \\ & - k_1[\text{H}^+]_0[\text{Br}^-][\text{HOBr}] + k_{-1}[\text{Br}_2] \\ & - k_2[\text{H}^+]_0[\text{Br}^-][\text{HBrO}_2] \\ & + k_0([\text{Br}^-]_0 - [\text{Br}^-]) \end{aligned} \quad (13)$$

The curve, g, in Fig. 1 shows the relationship between  $[\text{Br}^-]_0$  and  $[\text{Br}^-]_{ss}$  calculated by using Eqs. 10–13 when  $[\text{BrO}_3^-]_0 = 0.002 \text{ mol dm}^{-3}$ ,  $[\text{H}^+]_0 = 1.5 \text{ mol dm}^{-3}$ , and  $k_0 = 0.004 \text{ s}^{-1}$ . The curve suggests that the four-variable model is essentially equal to the FKN reaction scheme. In order to reduce the number of independent variables to two, we adopt the approximation that  $d[\text{Br}_2]/dt = 0$  and  $d[\text{HBrO}_2]/dt = 0$  at all times according to Bar-Eli and Noyes.<sup>21)</sup> Thus, we can obtain the following equations:

$$[\text{Br}_2] = (k_1[\text{H}^+]_0/(k_0 + k_{-1}))[\text{Br}^-][\text{HOBr}] \quad (14)$$

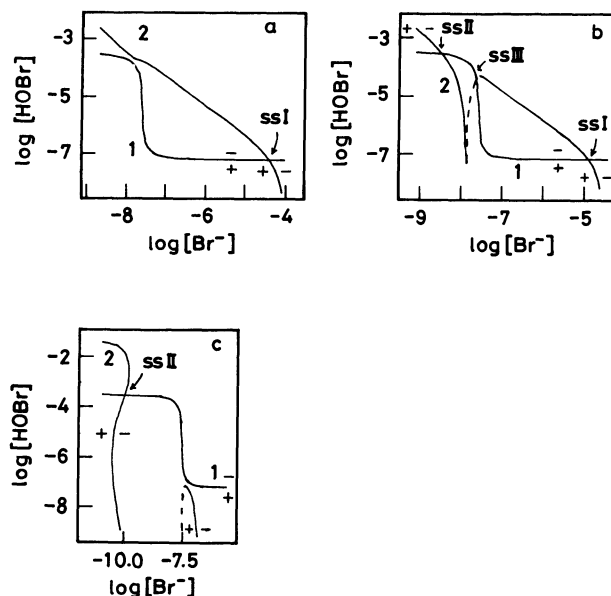


Fig. 5. Nullclines of the four-variable model.  $[\text{BrO}_3^-]_0 = 0.002 \text{ M}$ ,  $[\text{H}^+]_0 = 1.5 \text{ M}$ , and  $k_0 = 0.004 \text{ s}^{-1}$ .  $[\text{Br}^-]_0$  a:  $5 \times 10^{-4} \text{ M}$ , b:  $1.55 \times 10^{-4} \text{ M}$ , c:  $7 \times 10^{-7} \text{ M}$ . 1:  $d[\text{HOBr}]/dt = 0$ , 2:  $d[\text{Br}^-]/dt = 0$ . +:  $d[\text{HOBr}]/dt > 0$  or  $d[\text{Br}^-]/dt > 0$ , -:  $d[\text{HOBr}]/dt < 0$  or  $d[\text{Br}^-]/dt < 0$ .

$$\begin{aligned} [\text{HOBr}] = & (k_3[\text{H}^+]_0^2[\text{BrO}_3^-]_0[\text{Br}^-] - k_2[\text{H}^+]_0[\text{Br}^-][\text{HBrO}_2] \\ & + k_5[\text{H}^+]_0[\text{BrO}_3^-]_0[\text{HBrO}_2] - k_0[\text{HBrO}_2] \\ & - 2k_4[\text{HBrO}_2]^2)/(k_{-3}[\text{HBrO}_2]) \end{aligned} \quad (15)$$

A domain of  $[\text{HBrO}_2]$  where  $[\text{HBrO}_2] > 0$  and  $[\text{HOBr}] > 0$ , is defined from Eq. 15. We can depict the trajectory of the model system by using Eqs. 12–15.

Figure 5 shows the dependency of the HOBr and  $\text{Br}^-$  nullclines on  $[\text{Br}^-]_0$  when  $[\text{BrO}_3^-]_0 = 0.002 \text{ mol dm}^{-3}$ ,  $[\text{H}^+]_0 = 1.5 \text{ mol dm}^{-3}$  and  $k_0 = 0.004 \text{ s}^{-1}$ . In Fig. 5b ( $[\text{Br}^-]_0 = 1.55 \times 10^{-4} \text{ mol dm}^{-3}$ ), there are three intersections, i.e., three steady states (two stable nodes and one saddle point). Because the  $\text{Br}^-$  nullcline has an S-shape, interesting circumstances occur. In the left side of the  $\text{Br}^-$  nullcline,  $d[\text{Br}^-]/dt > 0$  and a state of the model system in the region varies temporally to the right. A state in the right side of the  $\text{Br}^-$  nullcline moves to the left for a similar reason. Therefore, the solid lines in the  $\text{Br}^-$  nullcline are stable because a state of the model system moves temporally toward the solid lines. On the other hand, the dashed line is unstable because a state of the model system temporally goes away from the dashed line. Thus, the middle intersection corresponds to an unstable steady state (saddle point) and the intersections of both sides to stable steady states (stable nodes). There is a separatrix through the saddle point, which separates the basins of attraction associated with the nodes. When the model system in a steady state is perturbed to pass the separatrix, the system relaxes to the other

steady state. On the other hand, Figs. 5a and c correspond to the case that the system has one stable steady state. Figures 5a–c suggest that at a critical value of  $[\text{Br}^-]_0$ , the nullclines yield one intersection and one point of contact and that at the  $[\text{Br}^-]_0$ , the model system jumps to the other steady state.

The four-variable model gives dynamical information on bistability in the bromate–bromide–cerium(III) system, but the oscillatory state in the model system has not yet been found at present.

#### References

- 1) W. Geiseler and H. H. Föllner, *Biophys. Chem.*, **6**, 107 (1977).
  - 2) W. Geiseler and K. Bar-Eli, *J. Phys. Chem.*, **85**, 908 (1981).
  - 3) W. Geiseler, *Ber. Bunsenges. Phys. Chem.*, **86**, 721 (1982).
  - 4) K. Bar-Eli and W. Geiseler, *J. Phys. Chem.*, **87**, 3769 (1983).
  - 5) R. J. Field, E. Körös, and R. M. Noyes, *J. Am. Chem. Soc.*, **94**, 8649 (1972).
  - 6) K. Bar-Eli and R. M. Noyes, *J. Phys. Chem.*, **81**, 1988 (1977).
  - 7) K. Bar-Eli and R. M. Noyes, *J. Phys. Chem.*, **82**, 1352 (1978).
  - 8) K. Bar-Eli, "Nonlinear Phenomena in Chemical Dynamics," ed by C. Vidal and A. Pacault, Springer-Verlag, West Berlin (1981), pp. 228–239.
  - 9) K. Bar-Eli and J. Ronkin, *J. Phys. Chem.*, **88**, 2844 (1984).
  - 10) Z. Noszticzius, E. Noszticzius, and Z. A. Schelly, *J. Phys. Chem.*, **87**, 510 (1983).
  - 11) F. Ariese and Z. Ungvárai-Nagy, *J. Phys. Chem.*, **90**, 1 (1986).
  - 12) F. Ariese and Z. Ungvárai-Nagy, *J. Phys. Chem.*, **90**, 1496 (1986).
  - 13) R. J. Field and H. -D. Försterling, *J. Phys. Chem.*, **90**, 5400 (1986).
  - 14) J. J. Tyson, "Oscillations and Traveling Waves in Chemical Systems," ed by R. J. Field and M. Burger, Wiley-Interscience, New York (1985), p. 95.
  - 15) S. Barkin, M. Bixon, R. M. Noyes, and K. Bar-Eli, *Int. J. Chem. Kinet.*, **9**, 841 (1977).
  - 16) R. J. Field and P. M. Boyd, *J. Phys. Chem.*, **89**, 3707 (1985).
  - 17) C. W. Gear, "Numerical Initial Value Problems in Ordinary Differential Equations," Prentice-Hall, Englewood Cliffs, N. J. (1971), Chap. 11.
  - 18) P. Grandsorff and I. Prigogine, "Thermodynamic Theory of Structure, Stability, and Fluctuations," Wiley-Interscience, New York (1971).
  - 19) J. H. Woodson and H. A. Liebhafsky, *Anal. Chem.*, **41**, 1894 (1969).
  - 20) G. J. Kasperek and T. C. Bruice, *Inorg. Chem.*, **10**, 382 (1971).
  - 21) K. Bar-Eli and R. M. Noyes, *J. Chem. Phys.*, **86**, 1927 (1987).
-